

Raman Marker Bands for *In-situ* Quality Control During Synthesis Of Two-Dimensional Conjugated Metal-Organic Frameworks

Fanny Reichmayr,^[a] Daniel Wolf,^[b] Geping Zhang,^[c] Mingchao Wang,^[c] Max Herzog,^[b] Renhao Dong,^[c,d] Xinliang Feng,^[c,e] Axel Lubk,^[b,f] Inez M. Weidinger^{*[a]}

[a] Fanny Reichmayr, Prof. Dr. Inez M. Weidinger

Chair of Electrochemistry, Faculty of Chemistry and Food Chemistry
Technische Universität Dresden
Zellescher Weg 19, 01069 Dresden, Germany
E-mail: inez.weidinger@tu-dresden.de

[b] Max Herzog, Dr. Daniel Wolf, Prof. Dr. Axel Lubk,

Leibniz Institut for Solid State and Materials Research Dresden
Helmholzstraße 20, 01069 Dresden, Germany

[c] Dr. Geping Zhang, Dr. Mingchao Wang, Prof. Dr. Renhao Dong, Prof. Dr. Xinliang Feng

Chair of Molecular Functional Materials, Faculty of Chemistry and Food Chemistry
Technische Universität Dresden
Mommsenstraße 4, 01069 Dresden, Germany

[d] Prof. Dr. Renhao Dong

Key Laboratory of Colloid and Interface Chemistry of the Ministry of Education, School of Chemistry and Chemical Engineering
Shandong University
Jinan, 250100, China

[e] Prof. Dr. Xinliang Feng

Max-Planck-Institut of Microstructure Physics
Weinberg 2, 06120 Halle/Saale, Germany

[f] Prof. Dr. Axel Lubk

Institute of Solid State and Materials Physics
Technische Universität Dresden
Haeckelstr. 3, 01069 Dresden, Germany

Abstract: Two-dimensional conjugated metal-organic frameworks (2D c-MOFs) are a subclass of MOFs that are of particular interest for electrocatalysis due to their good intrinsic conductivity. The electrochemical properties of such 2D frameworks are strongly related to their structure, which in turn is influenced by the synthesis conditions. However, even under formally identical conditions, MOF crystals with different structural properties are obtained, and to date there is no easy-to-apply method to predict the quality of MOF crystals already during synthesis. In the present work, we monitored the formation of phthalocyanine-based 2D MOFs at the air-water interface using *in-situ* Raman spectroscopy and identified Raman marker bands that characterise the degree of linker aggregation, the reaction progress, and the yield of MOFs formed during the reaction. Using transmission electron microscopy (TEM) measurements on the MOF crystals after synthesis, a correlation between the Raman marker bands and the resulting crystalline domain size distribution of the MOF could be derived. Thus, a method for a non-invasive, fast and simple *in-situ* quality assessment of the synthesised MOFs was established. These results are an important step towards the automation of MOF synthesis.

Metal-organic frameworks (MOFs) are a class of highly porous, crystalline solids that form a modular structure of metal centres^[1] and organic linkers^[2] via coordinative bonds.^[1-3] Their tunability enables application-specific customisation of their properties, leading to a wide range of applications such as gas storage,^[4] gas separation,^[5] sensing^[6] and (electro-)catalysis.^[7,8] The subclass of two-dimensional conjugated metal-organic frameworks (2D c-

MOFs) is of particular interest for use in electro-catalysis as they overcome the intrinsically low conductivity of conventional MOFs.^[3] This is because of their in-plane π -delocalisation along 2D directions and out-of-plane π - π -stacking.^[9] Due to the evident relationship between the structure and electrochemical performance of such 2D conjugated frameworks, a major focus of research is improving and controlling the crystalline domain size.^[10] Gaining a mechanistic understanding of the relationships between the synthesis conditions and the resulting structure and size is important to further improve the rational design of MOF materials and to gain a certain degree of predictability.^[11] With a deeper understanding of the reaction mechanisms, a basis for further optimisation approaches can be established and new insights into possible influences of synthesis conditions on reproducibility can be gained, ultimately paving the way towards automated processes. *In-situ* measurements are well suited to provide insights into reaction mechanisms and molecular interactions during syntheses. Furthermore, they can lead to conclusions about indicators for the quality of the synthesised MOF, forming an important step towards synthesis automation. Reported *in-situ* measuring methods investigating MOF syntheses include *in-situ* X-ray diffraction (XRD),^[12] *in-situ* nuclear magnetic resonance (NMR),^[13] *in-situ* time resolved static light scattering (TLS),^[14] *in-situ* liquid cell transmission electron microscopy (LCTEM),^[15] *in-situ* atomic force microscopy (AFM),^[16] *in-situ* extended X-ray absorption fine structure (EXAFS),^[17] and *in-situ* Raman spectroscopy.^[18] The great advantage of performing *in-situ* Raman spectroscopy is that it

allows chemical reactions and formation steps to be observed directly, even before MOF crystals are formed. It is also a fast and high-throughput technique, which can be applied during automated synthesis for quality control. On the other hand, spectra obtained with Raman spectroscopy are often ambiguous, especially for complex compounds such as MOFs. Therefore, complementary techniques (e.g. microscopy) must be used to verify the conclusions drawn from Raman spectroscopy before it can be used as a quality control application. The present work centres on the investigations of the structural dynamics during synthesis of the 2D c-MOF named $\text{Cu}_2[\text{ZnPc-O}_8]$, which consists of phthalocyaninato zinc linkers connected *via* copper bis(dioxolene) clusters. This $\text{Cu}_2[\text{ZnPc-O}_8]$ MOF is of interest as it is a known electro-catalyst for the hydrogen evolution reaction (HER) and CO_2 reduction reaction (CO₂RR).^[8] This MOF synthesis is particularly suitable for automated *in-situ* Raman measurements, as it is carried out under standard conditions at the water-air interface and thus requires no special measurement setup.^[19] Therefore, it is offering a considerable advantage over *in-situ* measurements in conventional MOF syntheses, which are carried out under solvothermal and high-temperature conditions. Extensive studies on phthalocyanines and phthalocyanine-based MOFs have been published, including resonance Raman investigations.^[20] It is therefore known that phthalocyanines have a tendency to aggregate in solution, especially in aqueous media.^[21] The aggregated and non-aggregated species can be differentiated with several spectroscopic methods, such as UV/VIS and Raman.^[22,23] While parallel oriented aggregates (H-type) show a blue shift in the spectra, head-to-head oriented aggregates (J-type) show a red-shift.^[23,24] In this work, we present how the aggregation tendencies of the phthalocyanine linker molecules on the water surface influence the synthesis and the final crystalline domain size distribution of the $\text{Cu}_2[\text{ZnPc-O}_8]$ MOF. This is substantiated with the analysis of appointed marker bands, which were recorded *in-situ* over the course of synthesis by means of resonance Raman. The insights obtained from the Raman spectra are compared with medium- and high-resolution TEM images to extract a correlation between Raman marker bands of the linker and the crystalline domain size distribution of obtained MOF sheets.

The synthesis of the two-dimensional conjugated metal-organic framework (2D c-MOF) $\text{Cu}_2[\text{ZnPc-O}_8]$, investigated in this work, was carried out at the water-air interface, according to the previous publication by Wang et al.^[19] For this purpose, the 2,3,9,10,16,17,23,24-octahydroxy phthalocyaninato Zn (ZnPc(OH)_8) linker molecules were dissolved in a chloroform/DMF solution and spread on the water surface where they formed a green film. The modulator sodium acetate (NaAcO) and the reactant copper(II) acetate ($\text{Cu}(\text{AcO})_2$) were then added to the water subphase in order to react with the linker to form the $\text{Cu}_2[\text{ZnPc-O}_8]$ MOF. Well-resolved Raman spectra were successfully measured from both the ZnPc(OH)_8 linker and the $\text{Cu}_2[\text{ZnPc-O}_8]$ MOF with a measurement time of only 1 min. As significant changes in the Raman spectra occurred in the first 10–30 min of synthesis, this allowed *in-situ* monitoring of the synthesis without the need to use ultra-fast methods. The

synthesis process including the *in-situ* Raman measurements is depicted in Figure 1.

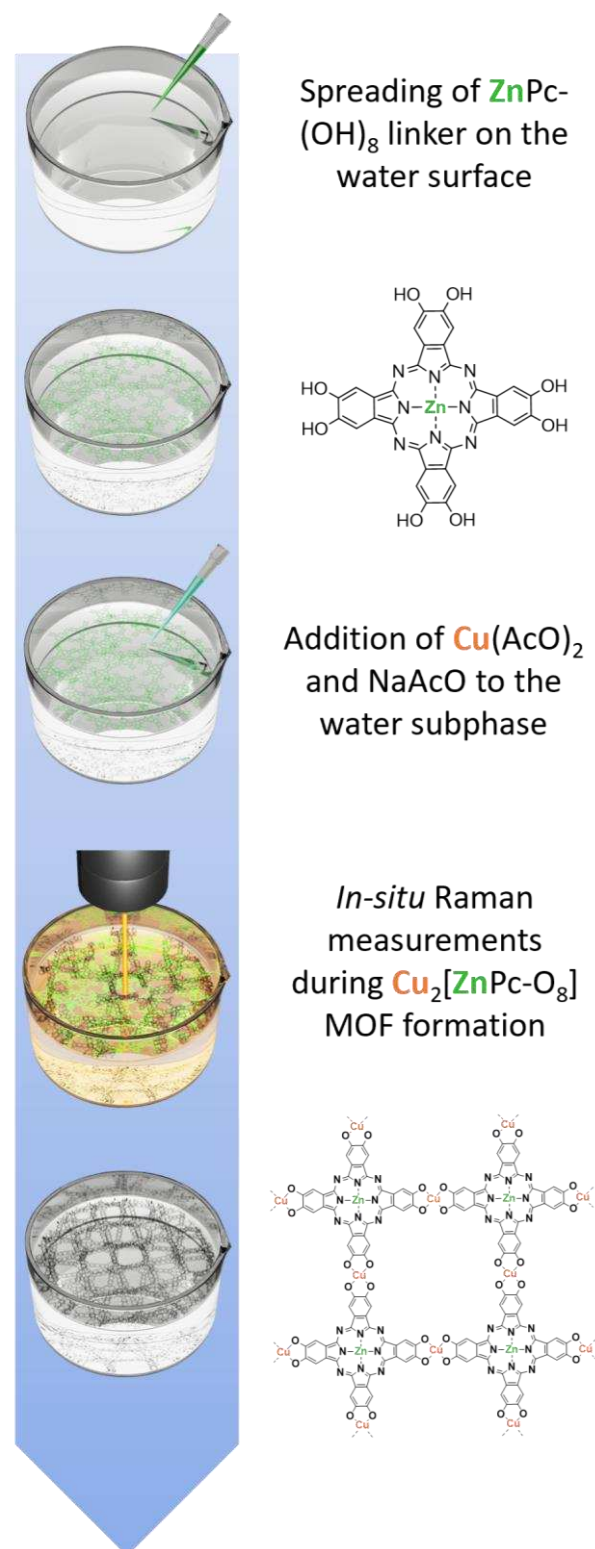


Figure 1. Depiction of $\text{Cu}_2[\text{ZnPc-O}_8]$ MOF synthesis and *in-situ* Raman. Before initiating the synthesis, a Raman spectrum of the ZnPc(OH)_8 linker molecules is measured on the water surface. Then, after adding $\text{Cu}(\text{AcO})_2$ and NaAcO , a spectrum is measured every minute. The linker spectrum measured before

the synthesis is already of great importance since changes in the Raman spectrum can be observed if the ZnPc-(OH)_8 linkers remain on the water surface for a longer period of time. Figure 2a shows how the Raman spectrum of the linker changes over time if left on the water surface for two hours. In detail, it can be seen that the intensity of the peak at 1491 cm^{-1} decreases over time, while the peak at 1514 cm^{-1} increases. As mentioned before, such a shift in the Raman spectrum is likely caused by aggregation, i.e. stacking of the phthalocyanines.^[22] The blue shift of approximately 20 cm^{-1} observed in the Raman spectra suggests that the linker molecules could aggregate in the so-called H-type stacking.^[23,24] A possible depiction of this is illustrated in Figure 2b. This conclusion is supported by the fact that the phthalocyanines arrange themselves perpendicular to the water surface,^[19] thus face-to-face stacking should be favoured. In the following, the peak at 1491 cm^{-1} is referred to as $\tilde{\nu}_{lin}$ as an indicator for the non-aggregated linker species and the peak at 1514 cm^{-1} as $\tilde{\nu}_{a.lin}$ for the aggregated linker species.

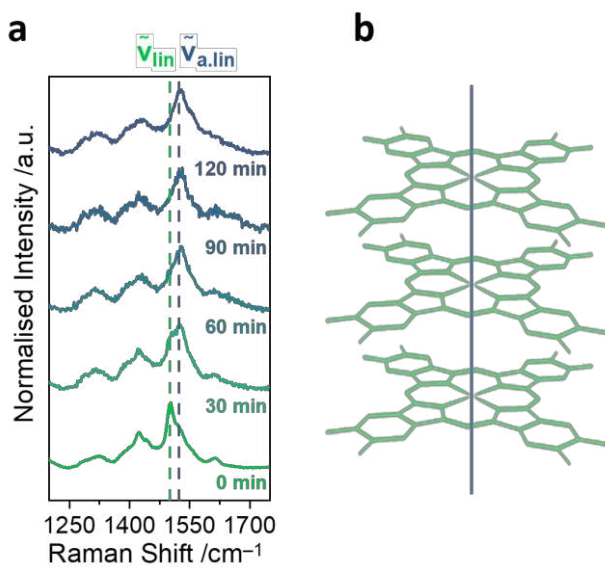


Figure 2. (a) Raman spectra of ZnPc-(OH)_8 linker on the water surface, measured at 594 nm ; (b) Depiction of the probable possible H-type stacking of ZnPc-(OH)_8 linker molecules.

From resonance Raman measurements and UV/VIS spectroscopy (Figure S1 and S3) it was further corroborated that aggregated ZnPc-(OH)_8 linker molecules show stronger resonance in the lower-energy region, while the resonance for the non-aggregated molecules lies in the higher-energy region. Therefore, the excitation laser wavelength of 594 nm was chosen for all further Raman measurements, as this enables the easy detection of both $\tilde{\nu}_{lin}$ and $\tilde{\nu}_{a.lin}$.

Figure 3a compares the Raman spectra of ZnPc-(OH)_8 linker and $\text{Cu}_2[\text{ZnPc-O}_8]$ MOF measured on the water surface. There are some clearly recognisable differences between the two Raman spectra. For reasons of clarity, however, the comparison and evaluation is based on the most intense peak in the MOF spectrum, which lies at 1506 cm^{-1} and is referred to as $\tilde{\nu}_{MOF}$. Interestingly, $\tilde{\nu}_{lin}$ is no longer found in the Raman spectrum of the MOF while $\tilde{\nu}_{a.lin}$ is still present, suggesting a residue of

aggregated linker molecules in the MOF sample (*vide infra*). Transmission Electron Microscopy (TEM) images of linker and MOF crystals are shown in Figure 3c and 3e. Although both have an oval shape and a comparable size, the MOF can still be distinguished from the linker, as the linker sheets have smooth edges while the MOF sheets are frayed. The energy dispersive X-ray (EDX) measurements, shown in Figure 3d and 3f, support this distinction with the Cu:Zn ratio, which is greater in the MOF material than in the linker compound. Note the fact that Cu is measured also in the linker compound is due to the presence of the copper TEM grid used here. Moreover, linker and MOF sheets can be distinguished by their different lattice spacings (Figure S5). The changes in the Raman spectra over the course of the synthesis can be viewed in Figure 3b. It is well recognisable that $\tilde{\nu}_{lin}$ and other prominent linker peaks such as the one at approximately 700 cm^{-1} disappear over time, while $\tilde{\nu}_{MOF}$ and other prominent MOF peaks such as the two between 1200 cm^{-1} and 1400 cm^{-1} emerge.

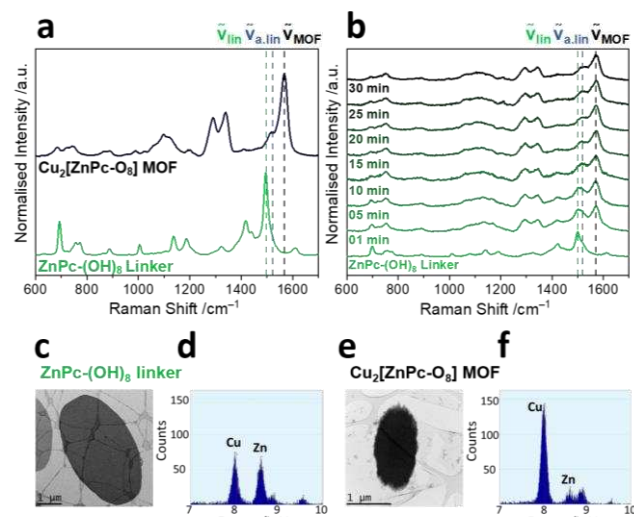


Figure 3. (a) Comparison of the Raman spectra of ZnPc-(OH)_8 linker (green) and $\text{Cu}_2[\text{ZnPc-O}_8]$ MOF (black) on the water surface measured at 594 nm ; (b) Raman measurements before and during $\text{Cu}_2[\text{ZnPc-O}_8]$ MOF synthesis on the water surface measured at 594 nm ; (c) TEM image of ZnPc-(OH)_8 linker sheets; (d) EDX measurements of ZnPc-(OH)_8 linker; (e) TEM image of $\text{Cu}_2[\text{ZnPc-O}_8]$ MOF sheets; (f) EDX measurements of $\text{Cu}_2[\text{ZnPc-O}_8]$ MOF.

To better visualise the changes in peak intensities over the course of the synthesis, the fitted peak intensities of $\tilde{\nu}_{lin}$, $\tilde{\nu}_{a.lin}$ and $\tilde{\nu}_{MOF}$ were set in relation according to the following equation:

$$I(\tilde{\nu}_{rel,MOF}) = \frac{I(\tilde{\nu}_{MOF})}{I(\tilde{\nu}_{lin}) + I(\tilde{\nu}_{a.lin}) + I(\tilde{\nu}_{MOF})} \quad (1)$$

A typical progression of the related peak intensities during the MOF synthesis can be seen in Figure 4a. One can observe that the intensity of $\tilde{\nu}_{lin}$ decreases, while that of $\tilde{\nu}_{MOF}$ increases. However, the intensity of $\tilde{\nu}_{a.lin}$ does not change significantly during the course of the reaction. This leads to the conclusion that non-aggregated linker molecules are consumed for the MOF synthesis, while aggregated linker molecules are apparently not involved in the reaction. This is consistent with the previous

observation that the Raman spectrum of the MOF sample showed residues of aggregated linker molecules.

In order to examine the influence of the extent of linker aggregation on the MOF synthesis, *in-situ* Raman measurements of the synthesis were performed with different initial degrees of linker aggregation. The investigated aggregation times are 0 min, 120 min and 240 min. The results are shown in Figure 4a, 4b and 4c respectively. The previously described progressions of $\tilde{\nu}_{lin}$, $\tilde{\nu}_{MOF}$ and $\tilde{\nu}_{a.lin}$ remain the same. However, the final intensity of $\tilde{\nu}_{MOF}$ decreases with increased aggregation time of the linker, with the highest intensity being reached at the lowest extent of linker aggregation (0 min). With a longer aggregation time of 120 min, the final intensity of $\tilde{\nu}_{MOF}$ is lower and decreases even more with 240 min aggregated linker. This trend indicates that the yield of MOF crystals formed decreases with increasing degree of linker aggregation. The pertinent issue posed is whether linker aggregation only affects the amount of MOF synthesised or also the crystalline domain size distribution. To investigate this, TEM measurements were performed on MOFs synthesised with different initial degrees of linker aggregation. The lengths and widths of the MOF sheets were measured and the area (size) was determined using the geometric approximation of an ellipse (see Equation S1). The resulting size distributions including their Gaussian fit functions are shown in Figure 4e, 4f and 4g for the respective aggregation times.

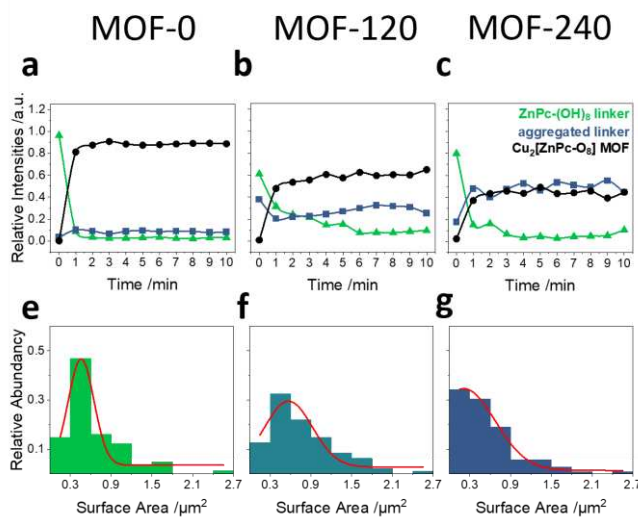


Figure 4. Relative Raman intensities over the reaction course of MOF synthesis with linker aggregation time of: (a) 0 min; (b) 120 min; (c) 240 min; size distribution of MOF synthesised with linker aggregation time of: (e) 0 min; (f) 120 min (g) 240 min.

The normal distributions provide a deeper insight into the influence of linker aggregation on the size distributions. They are referred to as $N_{MOF}(\mu; \sigma^2)$ with μ being the mean and σ^2 the variance of the function. MOFs synthesised at 0 min linker aggregation have a mean area of $0.46 \mu\text{m}^2$ with a small variance $N_0(0.46; 0.20)$. The normal distribution of MOFs synthesised at 120 min ($N_{120}(0.57; 0.68)$) show a slightly larger mean area, however the variance is more than three times as large. At the highest linker aggregation time of 240 min ($N_{240}(0.21; 1.18)$), the variance of the size distribution of the MOFs is even greater and

the mean size drops to $0.21 \mu\text{m}^2$. Therefore, a short linker aggregation time is preferable to obtain the largest possible MOFs with the narrowest possible size distribution. This observation from TEM measurements complements the results obtained from Raman measurements. In conclusion, the linker aggregation correlates directly with the yield and size distribution of the MOFs, but only at high aggregation times is the mean size also affected.

In this work the synthesis of the $\text{Cu}_2[\text{ZnPc-O}_8]$ MOF, performed on the water surface, was investigated by *in-situ* Raman spectroscopy. A correlation was revealed between the aggregation tendencies of the ZnPc(OH)_8 linker molecules, the yield and the crystalline domain size distribution of the synthesised MOF. A comparison with TEM images confirmed that the variance of the crystalline domain size distribution of the resulting $\text{Cu}_2[\text{ZnPc-O}_8]$ MOF sheets is larger the higher the degree of linker aggregation. At a very high aggregation time, even the average size of the MOFs decreases. It was shown that marker bands in the Raman spectra, which provide direct information about the yield and the size distribution of the MOFs, were successfully appointed. By correlating the intensities of the marker bands $\tilde{\nu}_{lin}$, $\tilde{\nu}_{a.lin}$ and $\tilde{\nu}_{MOF}$, *in-situ* Raman spectroscopy provides a non-invasive, quick and easy quality assessment of the synthesised MOFs. Thus, Raman spectroscopy was successfully introduced as a non-invasive *in-situ* method to monitor the quality of the synthesised $\text{Cu}_2[\text{ZnPc-O}_8]$ -MOF.

Supporting Information

The data supporting the findings of this study are available in the supplementary material.

Acknowledgements

The authors gratefully acknowledge financial support from the Collaborative Research Center "Chemistry of Synthetic 2D Materials" funded by the Deutsche Forschungsgemeinschaft (DFG, German Research Foundation) – SFB-1415 (417590517).

Keywords: *in-situ* spectroscopy • metal-organic frameworks • quality control • Raman spectroscopy • two-dimensional frameworks

- [1] C. S. Diercks, M. J. Kalmutzki, N. J. Diercks, O. M. Yaghi, *ACS Cent. Sci.* **2018**, *4*, 1457.
- [2] H. Furukawa, K. E. Cordova, M. O'Keeffe, O. M. Yaghi, *Science* **2013**, *341*, 1230444.
- [3] A. Schneemann, R. Dong, F. Schwotzer, H. Zhong, I. Senkovska, X. Feng, S. Kaskel, *Chem. Sci.* **2021**, *12*, 1600.
- [4] L. J. Murray, M. Dincă, J. R. Long, *Chem. Soc. Rev.* **2009**, *38*, 1294.
- [5] S. Kolkowitz, A. C. B. Jayich, Q. P. Unterreithmeier, S. D. Bennett, P. Rabl, J. G. E. Harris, M. D. Lukin, *Science* **2012**, *335*, 1603.
- [6] L. E. Kreno, K. Leong, O. K. Farha, M. Allendorf, R. P. van Duyne, J. T. Hupp, *Chem. Rev.* **2012**, *112*, 1105.
- [7] L. Jiao, Y. Wang, H.-L. Jiang, Q. Xu, *Adv. Mater.* **2018**, *30*, e1703663.
- [8] H. Zhong, M. Ghorbani-Asl, K. H. Ly, J. Zhang, J. Ge, M. Wang, Z. Liao, D. Makarov, E. Zschech, E. Brunner et al., *Nature communications* **2020**, *11*, 1409.
- [9] K. Zhao, W. Zhu, S. Liu, X. Wei, G. Ye, Y. Su, Z. He, *Nanoscale Adv.* **2020**, *2*, 536.

[10] a) K. Liu, H. Qi, R. Dong, R. Shihhare, M. Addicoat, T. Zhang, H. Sahabudeen, T. Heine, S. Mannsfeld, U. Kaiser et al., *Nature chemistry* **2019**, *11*, 994; b) M. Yu, R. Dong, X. Feng, *J. Am. Chem. Soc.* **2020**, *142*, 12903; c) J.-H. Dou, M. Q. Arguilla, Y. Luo, J. Li, W. Zhang, L. Sun, J. L. Mancuso, L. Yang, T. Chen, L. R. Parent et al., *Nature materials* **2021**, *20*, 222.

[11] A. K. Cheetham, G. Kieslich, H. H.-M. Yeung, *Acc. Chem. Res.* **2018**, *51*, 659.

[12] a) R. El Osta, M. Feyand, N. Stock, F. Millange, R. I. Walton, *Powder Diffr.* **2013**, *28*, S256-S275; b) F. Millange, R. El Osta, M. E. Medina, R. I. Walton, *CrystEngComm* **2011**, *13*, 103.

[13] M. Haouas, C. Volkrieger, T. Loiseau, G. Férey, F. Taulelle, *Chem. Mater.* **2012**, *24*, 2462.

[14] S. Hermes, T. Witte, T. Hikov, D. Zacher, S. Bahnmüller, G. Langstein, K. Huber, R. A. Fischer, *J. Am. Chem. Soc.* **2007**, *129*, 5324.

[15] J. P. Patterson, P. Abellán, M. S. Denny, C. Park, N. D. Browning, S. M. Cohen, J. E. Evans, N. C. Gianneschi, *J. Am. Chem. Soc.* **2015**, *137*, 7322.

[16] M. Shoaee, M. W. Anderson, M. P. Atfield, *Angew. Chem. Int. Ed.* **2008**, *47*, 8525.

[17] S. Surblé, F. Millange, C. Serre, G. Férey, R. I. Walton, *Chem. Commun.* **2006**, 1518.

[18] a) H. Embrechts, M. Kriesten, M. Ermer, W. Peukert, M. Hartmann, M. Distaso, *RSC Adv.* **2020**, *10*, 7336; b) H. Embrechts, M. Kriesten, K. Hoffmann, W. Peukert, M. Hartmann, M. Distaso, *J. Phys. Chem. C* **2018**, *122*, 12267.

[19] Z. Wang, L. S. Walter, M. Wang, P. S. Petkov, B. Liang, H. Qi, N. N. Nguyen, M. Hambach, H. Zhong, M. Wang et al., *J. Am. Chem. Soc.* **2021**, *143*, 13624.

[20] a) A. J. Bovill/A. A. McConnell/J. A. Nimmo/W. E. Smith, *J. Phys. Chem.* **1986**, 569; b) D. R. Tackley, G. Dent, W. Ewen Smith, *Phys. Chem. Chem. Phys.* **2001**, *3*, 1419; c) H. Abramczyk, I. Szymczyk, G. Waliszewska, A. Lebioda, *J. Phys. Chem. A* **2004**, *108*, 264; d) J. Jia, X. Zhao, W. Hu, Y. Wang, J. Huang, J. Huang, H. Li, Y. Peng, H. Ma, C. Xu, *J. Mater. Chem. A* **2023**, *11*, 8141; e) H. Zhong, K. H. Ly, M. Wang, Y. Krupskaya, X. Han, J. Zhang, J. Zhang, V. Kataev, B. Büchner, I. M. Weidinger et al., *Angew. Chem. Int. Ed.* **2019**, *58*, 10677; f) A. M. Dominic, Z. Wang, A. Kuc, P. Petkov, K. H. Ly, T. L. H. Pham, M. Kutzschbach, Y. Cao, J. Bachmann, X. Feng et al., *J. Phys. Chem. C* **2023**, *127*, 7299.

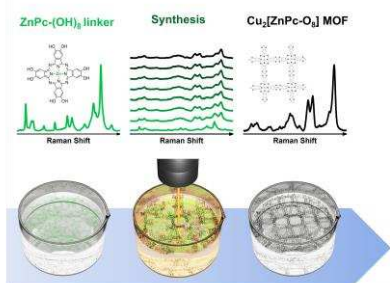
[21] a) J. R. Darwent, P. Douglas, A. Harriman, G. Porter, M.-C. Richoux, *Coordination Chemistry Reviews* **1982**, 83; b) T. Nyokong, *Coordination Chemistry Reviews* **2007**, *251*, 1707.

[22] B. Brożek-Pluska, I. Szymczyk, H. Abramczyk, *Journal of Molecular Structure* **2005**, 744-747, 481.

[23] K. Palewska, J. Sworakowski, J. Lipiński, *Optical Materials* **2012**, *34*, 1717.

[24] M. Kasha, *Radiation research* **2012**, *178*, AV27-34.

Entry for the Table of Contents



The properties of two-dimensional conjugated metal-organic frameworks (2D c-MOFs) are related to their structure and are influenced by the synthesis conditions. Here, we used *in-situ* Raman and transmission electron microscopy (TEM) to determine Raman marker bands that characterise the reaction progress and yield of phthalocyanine-based 2D Cu₂[ZnPc-O₈] MOFs. Thus, a non-invasive quality assessment method of the synthesised MOFs was established.